Self-assembled Films of Prussian Blue and Analogues: Optical and Electrochemical Properties and Application as Ion-Sieving Membranes

Mario Pyrasch, Ali Toutianoush, Wanqin Jin, Judit Schnepf, and Bernd Tieke*

Institut für Physikalische Chemie, Universität zu Köln, Luxemburger Str. 116, D-50939 Köln, Germany

Received June 11, 2002. Revised Manuscript Received October 4, 2002

Ultrathin films of metal hexacyanometalates were prepared upon multiple sequential adsorption of metal cations M^{m+} (Fe^{3+}, Fe^{2+}, Co^{2+}, and Ni^{2+}) and hexacyanometalate anions $[M(CN)_6]^{n-}$ ($Fe(CN)_6^{3-}$, $Fe(CN)_6^{4-}$, and $Co(CN)_6^{3-}$) on solid supports. The layer-by-layer deposition led to the formation of films of the metal complex salts with monolayer precision. The films were characterized using UV and IR spectroscopic methods and cyclic voltammetry. The alternating adsorption of Fe^{3+} and $Fe(CN)_6^{4-}$ ions led to dense and defect-free films of Prussian Blue, which were useful as membranes for ion separation. The porous, zeolitic structure of Prussian Blue was permeable for ions with a small Stokes radius such as Cs^+, K^+, and Cl^-, whereas large hydrated ions such as Na^+, Li^+, Mg^{2+}, or SO_4^{2-} were blocked. The effect of ion sieving increased with the thickness of the membrane. After a hundred dipping cycles, high separation factors α(CsCl/NaCl) and α(KCl/NaCl) of 6.5 and 6.2, respectively, were found. Corresponding membranes of cobalt and nickel hexacyanoferrate were also useful for ion separation, but the α-values were lower. Possible reasons for the differences in selectivity are discussed.

1. Introduction

Prussian Blue (PB)[1] is the prototype compound of a number of mixed valence hexacyanometalate salts[2,3] with interesting electrochemical,[4] electrochromic,[5] photophysicalm[6] and magnetic properties[7] and potential analytic applications.[8] These properties can only be fully exploited if thin films of the compounds are prepared. However, common techniques of film preparation such as electrochemical deposition,[9] casting from colloidal solution,[10] or dip-coating[11] are hampered by the fact that a precise control of the thickness in the nanometer range is lacking. This problem has recently been overcome by applying Langmuir−Blodgett (LB)[12] and self-assembly[13,14] deposition techniques. While the LB technique allows preparation of films consisting simultaneously of PB and amphiphiles,[12] the self-assembly technique based on multiple sequential adsorption (MSA) of ferric cations and hexacyanoferrate anions is well-suited for preparation of pure PB films with nanometer precision.[13,14] Using the same preparation technique, films of other mixed valence salts such as Ruthenium Purple[14] or copper hexacyanoferrate[15] have also been prepared.

The present article is an extension of our previous work[14] on ultrathin films of PB prepared using the MSA technique. Here, we report on preparation and characteristic properties of a variety of related films such as Prussian Yellow (PY) and Everitt's salt (Prussian White), cobalt and nickel hexacyanoferrate, and iron hexacyanocobaltate and compare the properties with those of PB films. The characteristic properties such as optical absorption and electrochemical properties were investigated using UV/visible and FTIR spectroscopy as well as cyclic voltammetry.

PB exhibits an open, zeolite-like structure consisting of a cubic framework of iron centers bound by cyanide bridges such that additional cations can intercalate into the interstitial sites and indefinite amounts of water can be included.[1,4] Because of the small channels in the lattice with a diameter of about 0.32 nm, small hydrated cations such as K^+, Rb^+, Cs^+, and NH_4^+ can penetrate the structure, while larger ions such as Na^+, Li^+, and

* To whom correspondence should be addressed.

(1) (a) Keggin, J. F.; Miles, F. D. *Nature (London)* **1936**, *137*, 577. (b) Ludi, A. *Chem. Unserer Zeit* **1988**, *23*, 123.
(2) Chadwick, B. M.; Sharpe, A. G. *Adv. Inorg. Chem. Radiochem.* **1966**, *8*, 83.
(3) Sharpe, A. G. *The Chemistry of Cyano Complexes of the Transition Metals*; Academic Press: New York, 1976.
(4) Itaya, K.; Uchida I.; Neff, V. D. *Acc. Chem. Res.* **1986**, *19*, 162.
(5) (a) Mortimer, R. J. *Chem. Soc. Rev.* **1993**, *26*, 147. (b) Kulesza, P. J.; Miecznikowski, K.; Chojak, M.; Malik, M. A.; Zamponi, S.; Marassi, R. *Electrochim. Acta* **2001**, *46*, 4371.
(6) Kaneko, M.; Hara, S., Yamada, A. *J. Electroanal. Chem.* **1985**, *194*, 165.
(7) Mingotaud, C.; Lafuente, C.; Amiell, J.; Delhaes, P. *Langmuir* **1999**, *15*, 289.
(8) (a) Koncki, R. *Critical Rev. Anal. Chem.* **2002**, *32*, 79. (b) Karyakin A. A. *Electroanalysis* **2001**, *13*, 813.
(9) (a) Itaya, K.; Ataka, T.; Toshima, S. *J. Am. Chem. Soc.* **1982**, *104*, 4767. (b) Lundgren, C. A.; Murray, R. W. *Inorg. Chem.* **1988**, *27*, 933. (c) Neff, V. D. *J. Electrochem. Soc.* **1985**, *132*, 1382. (d) Mortimer, R. J.; Rosseinsky, D. R. *J. Electroanal. Chem.* **1983**, *151*, 133.
(10) Toshima, N.; Liu, K.; Kaneko, M. *Chem. Lett.* **1990**, 485.
(11) Neff, V. D. *J. Electrochem. Soc.* **1978**, *125*, 886.
(12) Ravaine, S.; Lafuente, C.; Mingotaud, C. *Langmuir* **1998**, *14*, 6347.
(13) Millward, R. C.; Madden, C. E.; Sutherland, I.; Mortimer, R. J.; Fletcher, S.; Marken, F. *Chem. Commun.* **2001**, 1994.
(14) Pyrasch, M.; Tieke, B. *Langmuir* **2001**, *17*, 7706.
(15) Barathi, S.; Nogami, M.; Ikeda, S. *Langmuir* **2001**, *17*, 7468.

10.1021/cm021230a CCC: $25.00 © 2003 American Chemical Society
Published on Web 12/03/2002

all of the group II cations are blocked. Thin films of PB and related analogous complex salts are therefore interesting candidates for the preparation of separating membranes capable of ion sieving. In previous studies, size-selective transport of ions across PB-type films to an underlying electrode was investigated. The studies demonstrated the usefulness of the films as ion-selective electrodes,[16] electrocatalytic surfaces,[17] and ion exchangers.[18] In this work, size-selective transport of ions through self-assembled films of PB on porous polymer supports is reported, the transport being driven by a concentration gradient across the membrane. The studies are made possible by the fact that the MSA technique allows the preparation of the separating membrane with highly reproducible thickness, structure, and surface properties. First results are presented which demonstrate the utility of the resulting composite membranes for ion sieving.

2. Experimental Section

Materials. Potassium hexacyanoferrate(III), $K_3[Fe(CN)_6]\cdot 3H_2O$ (Fluka), potassium hexacyanoferrate(II), $K_4[Fe(CN)_6]\cdot 3H_2O$ (Fluka), ammonium ferrous sulfate, $(NH_4)_2Fe(SO_4)_2\cdot 6H_2O$ (Merck), ferric chloride, $FeCl_3\cdot 6H_2O$ (Acros), nickel(II) chloride, $NiCl_2\cdot 6H_2O$ (Merck), cobalt(II) chloride, $CoCl_2\cdot 6H_2O$ (Fluka), potassium hexacyanocobaltate(III), $K_3[Co(CN)_6]$ (Acros), and potassium chloride, KCl (Acros), were of analytical purity and used without further purification. Poly(styrene sulfonate), PSS, sodium salt (molecular weight 70 000), poly(diallyldimethylammonium chloride), PDADMA (molecular weight 250 000), and poly(allylamine hydrochloride), PAH (molecular weight from 50 000 to 65 000), were purchased from Aldrich and polyvinylamine, PVA (molecular weight 100 000) was kindly provided from BASF, Ludwigshafen. The polyelectrolytes were used for precoating of the substrates without further purification. Milli-Q-water (resistance ≥18.2 MΩ) was used for all experiments.

Pretreatment of Substrates. For deposition of the complex salts, pretreated quartz substrates (Suprasil, 30 × 12 × 1 mm, Vogelsberger Quarzglas, Sonnen), glass substrates coated with a 70-nm-thick layer of indium−tin oxide (ITO, Plano, Wetzlar, resistance 100 Ω-cm^{-2}), or PAN/PET membranes were used. The quartz substrates were cleaned upon washing with a common household detergent (anionic and nonionic surfactants) and subsequent ultrasonification in water at 60 °C for 30 min. Then the substrates were either immersed in a 1 wt % aqueous solution of PDADMA for 30 min[19] or in a 5 wt % solution of 3-aminopropyldimethoxymethylsilane (Fluka) in toluene for at least 12 h.[20] Subsequently, the substrates were alternately coated[21] with three layer pairs PSS and PAH, the uppermost layer being PAH. All polyelectrolytes were adsorbed from aqueous solutions containing 0.01 monomol/L of the polymer (monomol refers to a molar concentration of monomer units) and 0.01 M HCl.

The ITO-coated glass was cleaned upon washing with a common household detergent (anionic and nonionic surfactants) and subsequent ultrasonification in water at 60 °C for 30 min. Ultrasonic treatment was repeated three times. Then the substrate was either immersed in an aqueous PDADMA solution (concentration: 1 wt %) or precoated with three layer pairs of PSS/PAH, the uppermost layer being PAH.

As the porous support for the ion permeation studies, a technical PAN/PET membrane kindly supplied by Dr. A. Hübner, Sulzer Chemtech GmbH, Neunkirchen, was used. It consists of a poly(ethylene terephthalate) (PET) fleece (thickness 100 μm) coated with a polyacrylonitrile (PAN) layer (thickness 80 μm), the pore sizes being 20−200 nm. The surface was rendered hydrophilic by treatment with oxygen plasma and by subsequent dipping into a 0.01 M aqueous solution of PVA so that a monolayer of PVA was adsorbed. Then the complex salt was deposited.

Preparation of the Complex Salt Films. In Tables 1 and 2, the complex salts and their abbreviations, some details on film preparation, and characteristic film properties are listed.

Films of PB. $Fe^{III}HCF^{II}$ and $Fe^{II}HCF^{III}$ films were prepared using pretreated quartz or ITO coated glass substrates. For the $Fe^{II}HCF^{III}$ films, the substrates were alternately dipped into 0.01 M aqueous solutions of potassium HCF(III) and ammonium ferrous sulfate, while for the $Fe^{III}HCF^{II}$ films, the substrates were alternately dipped into 0.01 M aqueous solutions of potassium HCF(II) and ferric chloride. All solutions contained KCl in 0.5 M concentration. The substrates were kept in each solution for 30 min and subsequently washed with water before they were dipped into the next solution. In both cases, blue films are obtained upon the repeated dipping procedure.

Films of Everitt's Salt and PY. $Fe^{II}HCF^{II}$ and $Fe^{III}HCF^{III}$ films were prepared like the PB films except that other dipping solutions were used. $Fe^{II}HCF^{II}$ films were prepared upon alternate dipping of pretreated supports into 0.01 M aqueous solutions of potassium HCF(II) and ammonium ferrous sulfate, while $Fe^{III}HCF^{III}$ films were obtained from solutions of potassium HCF(III) and ferric chloride.

Films of Nickel Hexacyanoferrate. The films were prepared like the PB films except that other dipping solutions were used. $Ni^{II}HCF^{II}$ films were obtained from 0.01 M aqueous solutions of potassium HCF(II) and nickel(II) chloride, while $Ni^{II}HCF^{III}$ films were prepared from solutions of potassium HCF(III) and nickel(II) chloride.

Films of Cobalt Hexacyanoferrate. The films were prepared like the PB films except that other dipping solutions were used. $Co^{II}HCF^{II}$ films were obtained from 0.01 M aqueous solutions of potassium HCF(II) and cobalt(II) chloride, while $Co^{II}HCF^{III}$ films were prepared using solutions of potassium HCF(III) and cobalt(II) chloride.

Films of Iron Hexacyanocobaltate. The $Fe^{II}HCC^{III}$ films were prepared like the PB films except that 0.01 M aqueous dipping solutions of potassium HCC(III) and ammonium ferrous sulfate were used.

Preparation of the Membranes. *$Fe^{III}HCF^{II}$ Membranes.* After precoating with a monolayer of PVA, the PAN/PET membranes were first dipped into a 0.01 M aqueous solution of potassium HCF(II) followed by dipping into a 0.01 M aqueous solution of ferric chloride and so on. Both solutions contained KCl in 0.1 M concentration. After each dipping step the membrane was washed with water to remove nonadsorbed ions. The dipping time was 20 s and the washing time 1 min.

$Fe^{II}HCF^{III}$, $Ni^{II}HCF^{III}$, and $Co^{II}HCF^{III}$ Membranes. The preparation was according to the $Fe^{III}HCF^{II}$ membrane except that the aqueous solutions contained potassium HCF(III) and either ferrous chloride, nickel(II) chloride, or cobalt(II) chloride. The dipping time was 5 min and the washing time 10 min.

Methods. UV/visible absorption spectra were recorded using a Perkin-Elmer Lambda 14 spectrometer. All spectra were corrected by subtracting the signal of the pure quartz substrate. Fourier transform infrared (FTIR) spectra were recorded on a Perkin-Elmer Paragon 1000 spectrometer. Scanning force microscopic (SFM) images were taken with a Nanoscope IV SFM (Digital Instruments) working in contact mode. The samples were investigated in air at room temperature. The images were taken in equiforce mode, and com-

(16) Schneemeyer, L. F.; Spengler, S. E.; Murphy, D. W. *Inorg. Chem.* **1985**, *24*, 3044.
(17) (a) Itaya, K.; Shoji, N.; Uchida, I. *J. Am. Chem. Soc.* **1984**, *106*, 3423. (b) Shankaran, D. R.; Narayanan, S. S.; Fresenius, J. *Anal. Chem.* **1999**, *365*, 663.
(18) (a) Mardan, A.; Ajaz, R.; Mehmood, A.; Raza, S. M.; Ghaffar, A. *Sep. Purif. Technol.* **1999**, *16*, 147. (b) Green-Pedersen, H.; Korshin, G. V. *Environ. Sci. Technol.* **1999**, *33*, 2633. (c) Jeerage, K. M.; Schwartz, D. T. *Sep. Sci. Technol.* **2000**, *35*, 2375. (d) Lin, Y.; Fryxell, G. E.; H. Wu; Engelhard, M. *Environ. Sci. Technol.* **2001**, *35*, 3962.
(19) Kotov, N. A.; Dekany, I.; Fendler, J. H. *J. Phys. Chem.* **1995**, *99*, 13065.
(20) Moon, J. H.; Shin, J. W.; Kim, S. Y.; Park, J. W. *Langmuir* **1996**, *12*, 4621.
(21) Decher, G. *Science* **1997**, *277*, 1232.

mercially available Si/N cantilevers with integrated tips were used. Cyclic voltammetry was performed on a Heka (Heka electronic, Lambrecht, Germany) potentiostat/galvanostat (model PG 390). Data aquisition and potentiostat control were accomplished with a pentium 133 MHz IBM-compatible computer running the POTPULSE software (Heka), version 8.4. All experiments were carried out in a 500-mL three-electrode glass cell at room temperature employing the PB film on an ITO-coated glass substrate, a saturated calomel reference electrode (SCE), and a platinum plate (4 cm^2) as the counter electrode. The electrochemical experiments were carried out in 0.5 M aqueous KCl solution, pH 5.5, saturated with N_2. Cyclic voltammetric curves were recorded in the potential range from −200 to +1200, or +1000 mV, always beginning at −200 mV. The scan rate was 2.3 mV s^{-1}.

Studies of Ion Transport. Ion transport measurements were carried out using a homemade apparatus. The membrane of area A (=4.52 cm^2) was placed between two chambers with a volume V_0 of 60 mL each. The first chamber contained the aqueous electrolyte solution of 0.1 M concentration c, and the other chamber contained pure water and the cell for measurement of the conductivity Λ. The flux J of electrolytes across the membrane was determined by measuring the initial increase of conductivity $\Delta\Lambda$ per unit time Δt under constant stirring. The osmotic flow of water in the opposite direction was taken into account by measuring the volume increase ΔV in the first chamber during the time period Δt of the measurement. J was calculated from the equation $J = (\Delta\Lambda/\Delta t)(V_0 - \Delta V)(\Lambda_m A)^{-1}$ with Λ_m being the molar conductivity of the corresponding electrolyte solution. The change of the flux due to correction of the osmotic flow was never larger than 2%. The theoretical separation factor α is given by the ratio of the flux values J of the corresponding electrolyte solutions, for example, for the solutions of CsCl and NaCl $\alpha(\text{CsCl/NaCl}) = J(\text{CsCl})/J(\text{NaCl})$.

3. Results and Discussion

3.1. Films of Prussian Blue. As already described in a previous paper,[14] two different routes can be applied for preparation of PB films. According to the first route, the precoated substrate is consecutively dipped into an aqueous solution of potassium HCF(II) such that the HCF(II) anions are adsorbed followed by dipping into an aqueous ferric chloride solution to adsorb the Fe(III) cations and so on. As soon as the substrate was dipped into the ferric chloride solution, it turned blue, indicating the formation of a PB film, which we denote as $Fe^{III}HCF^{II}$ film. UV/visible absorption spectra of $Fe^{III}HCF^{II}$ films monitored after 12 dipping cycles are shown in Figure 1. They are dominated by the intense broad charge-transfer absorption band of the mixed valence $Fe^{II}-CN-Fe^{III}$ sequence with a maximum at 700 nm. The band intensity increases with the number of dipping cycles with only small deviations from linearity, indicating that in each dipping cycle nearly the same amount of material is added to the substrate (see inset of Figure 1).

The second route to PB films is based on the consecutive dipping of the pretreated substrates into aqueous solutions of potassium HCF(III) and ammonium ferrous sulfate. Again, the substrate turned deep blue, indicating the formation of a PB film, which is denoted as $Fe^{II}HCF^{III}$ film. The optical absorption spectrum of the film is slightly different from the $Fe^{III}HCF^{II}$ film. This is somewhat surprising because previous studies[22] on bulk

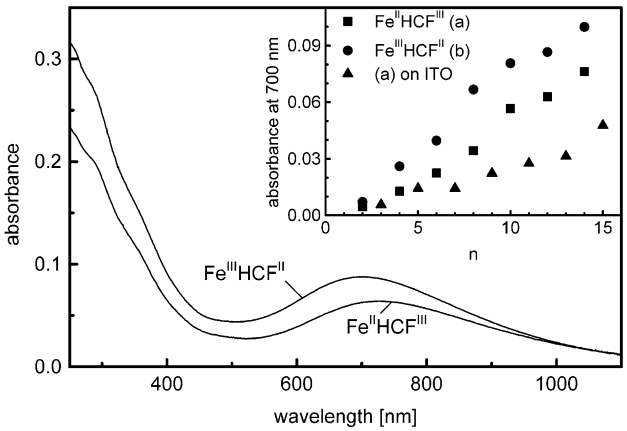

Figure 1. UV/visible absorption spectra of $Fe^{III}HCF^{II}$ and $Fe^{II}HCF^{III}$ films after 12 dipping cycles. The inset shows the absorbance of the films at λ_{max} = 700 nm as a function of the number n of dipping cycles. The influence of the substrate coating is also shown. Substrates: Quartz or ITO glass coated with three layer pairs PSS/PAH.

material have shown that the two preparation routes lead to compounds of identical chemical composition. As can be seen from the optical spectra of Figure 1, the two films show the same broad, intense charge-transfer band with a maximum at about 700 nm, but the optical density of the $Fe^{II}HCF^{III}$ film is clearly lower. The reason might be that in the $Fe^{II}HCF^{III}$ film ions of lower charge numbers ($z^+ = 2$ and $z^- = 3$) are adsorbed compared to those in the $Fe^{III}HCF^{II}$ film, where the charge numbers of the ions are $z^+ = 3$ and $z^- = 4$. Thus, in the latter case the surface charge is higher and more ions of opposite charge are adsorbed at the film surface. Consequently, the optical density per dipping step is higher. At low number of dipping cycles, both films exhibit an almost linear increase of the band intensity, whereas after more than 12 dipping cycles deviations from linearity occur. This indicates a change in the growth behavior, whose origin is not yet clear (see inset of Figure 1).

The formation of the metal hexacyanoferrate complex salt can also be detetected from FTIR spectra of the multilayers on glass substrates. The complex formation is accompanied by a shift of the C−N stretching mode from 2040 cm^{-1} in $K_4[Fe(CN)_6]\cdot 3H_2O$ and 2117 cm^{-1} in $K_3[Fe(CN)_6]\cdot 3H_2O$[23] to 2070 and 2080 cm^{-1} in the $Fe^{III}HCF^{II}$ and $Fe^{II}HCF^{III}$ films (see also Table 1), respectively, due to the change from the mono- to bidentate character of the cyano ligand group. The values for the self-assembled PB films are in agreement with those of chemically deposited films.[24]

The electrochemical behavior of the self-assembled PB films was reported previously.[14] A typical voltammogram of an $Fe^{III}HCF^{II}$ film prepared upon 20 dipping cycles exhibits two signals with mid-potentials at 200 and 880 mV vs SCE (not shown, see Table 2), in agreement with data from films of microcrystalline PB particles.[25] The oxidation/reduction signal at 200 mV

(22) (a) Fluck, E.; Kerler, W.; Neuwirth, W. *Angew. Chem., Int. Ed. Engl.* **1963**, *2*, 277. (b) Robin, M. B.; Day, P. *Adv. Inorg. Chem. Radiochem.* **1967**, *10*, 247.

(23) Sauter, S.; Wittstock, G.; Szargan, R. *Phys. Chem. Chem. Phys.* **2001**, *3*, 562.

(24) (a) Ellis, D.; Eckhoff, M.; Neff, V. D. *J. Phys. Chem.* **1981**, *85*, 1225. (b) Wilde, R. E.; Ghosh, S. N.; Marshall, B. J. *Inorg. Chem.* **1970**, *9*, 2512.

(25) Dostal, A.; Meyer, B.; Scholz, F.; Schröder, U.; Bond, A. M.; Marken, F.; Shaw, S. *J. Phys. Chem.* **1995**, *99*, 2096.

Table 1. List of Films and Some Characteristic Properties

denotation of film	0.01 M aqueous dipping solutions containing 0.5 M KCl		λ_{max} (nm)	$\nu_{C\equiv N}$ (cm^{-1})	notes
$Fe^{III}HCF^{II}$	$FeCl_3 \cdot 6H_2O$	$K_4[Fe(CN)_6] \cdot 3H_2O$	338 sh, 700	2070	Prussian Blue
$Fe^{II}HCF^{III}$	$(NH_4)_2Fe(SO_4)_2 \cdot 6H_2O$	$K_3[Fe(CN)_6] \cdot 3H_2O$	338 sh, 700	2080	Prussian Blue
$Fe^{III}HCF^{III}$	$FeCl_3 \cdot 6H_2O$	$K_3[Fe(CN)_6] \cdot 3H_2O$	338 sh	2111	Prussian Yellow
$Fe^{II}HCF^{II}$	$(NH_4)_2Fe(SO_4)_2 \cdot 6H_2O$	$K_4[Fe(CN)_6] \cdot 3H_2O$	287 sh		Everitt's salt
$Ni^{II}HCF^{III}$	$NiCl_2 \cdot 6H_2O$	$K_3[Fe(CN)_6] \cdot 3H_2O$	290, 380, 410 sh	2094, 2162	
$Ni^{II}HCF^{II}$	$NiCl_2 \cdot 6H_2O$	$K_4[Fe(CN)_6] \cdot 3H_2O$	302	2086	
$Co^{II}HCF^{III}$	$CoCl_2 \cdot 6H_2O$	$K_3[Fe(CN)_6] \cdot 3H_2O$	364 sh, 516	2109, 2188	
$Co^{II}HCF^{II}$	$CoCl_2 \cdot 6H_2O$	$K_4[Fe(CN)_6] \cdot 3H_2O$	370	2080	
$Fe^{II}HCC^{III}$	$(NH_4)_2Fe(SO_4)_2 \cdot 6H_2O$	$K_3[Co(CN)_6]$	363 sh, 500 sh	2161	
$Co^{II}HCC^{III}$	$CoCl_2 \cdot 6H_2O$	$K_3[Co(CN)_6]$[a]	*b*	2172	

[a] Deposition only from 0.1 M solutions. [b] Pink film, no maximum or shoulder in UV/visible region.

Table 2. Electrochemical Properties[a]

	E_{ox} (V) precoating:		E_{red} (V) precoating:		$(E_{ox} + E_{red})/2$ (V) precoating:	
denotation of film	PSS/PAH	PDADMA	PSS/PAH	PDADMA	PSS/PAH	PDADMA
$Fe^{II}HCF^{III}$	0.30/0.96	n.d.	0.09/0.79	n.d.	0.20/0.88	n.d.
$Fe^{III}HCF^{III}$	0.28/0.80	0.27/0.80	0.37/0.74	0.23/0.75	0.25/0.77	0.25/0.77
$Ni^{II}HCF^{III}$	0.67	n.d.	0.27	n.d.	0.47	n.d.
$Ni^{II}HCF^{II}$	0.49/0.65	0.48/0.64	0.41/0.57	0.45/0.62	0.45/0.61	0.47/0.62
$Co^{II}HCF^{III}$	0.77	0.71	0.52	0.54	0.65	0.63
$Co^{II}HCF^{II}$	0.57/0.77	0.51/0.71	0.32/0.66	0.44/0.67	0.45/0.72	0.48/0.69
$Fe^{II}HCC^{III}$	n.d.	0.81 (1. scan) 0.36 (2. scan)	n.d.	−0.06 −0.06	n.d.	n.d.

[a] n.d.: not determined.

originates from the $Fe^{II}HCF^{II}$/ $Fe^{III}HCF^{II}$ redox couple and the other one from the $Fe^{III}HCF^{II}$/ $Fe^{III}HCF^{III}$ couple.

3.2. Films of Prussian Yellow and Everitt's Salt. The MSA deposition of Fe(III) and HCF(III) ions yielded brown yellow, transparent films of PY, which we denote as $Fe^{III}HCF^{III}$ films. UV/visible spectra of these films monitored after different numbers of dipping cycles are shown in Figure 2a. The spectra indicate a shoulder at 338 nm, which strongly increases in absorbance, if the number *n* of dipping cycles becomes higher. The increase is rather linear up to about 12 dipping cycles, whereas at higher *n* values an exponential increase is observed.

The alternating deposition of Fe(II) cations and HCF-(II) anions resulted in a light blue film which in principle consists of Everitt's salt, here denoted as $Fe^{II}HCF^{II}$. The bluish color already appeared during film preparation and can be ascribed to partial oxidation of colorless Everitt's salt to PB under ambient conditions. Deposition of the films in a drybox in an inert atmosphere will probably allow the preparation of pure Everitt's salt films. UV/visible spectra of the films indicate a strong absorption in the UV with a shoulder at 287 nm, mainly originating from $Fe^{II}HCF^{II}$ and a weak absorption at 700 nm due to the presence of small amounts of Fe^{III}-HCF^{II} (not shown). The increase of absorbance with the number of dipping cycles is not linear. This may be caused by a weak adherence of the $Fe^{II}HCF^{II}$ crystallites to the substrate so that some material is leached out upon the repeated dipping.

The formation of PY is also indicated from the FTIR spectra of the self-assembled films. The C−N stretching frequency of the $Fe^{III}HCF^{III}$ film appears at 2111 cm^{-1}; that is, there is only a very small hypsochromic shift of 6 cm^{-1} compared to that of the starting compound $K_3[Fe(CN)_6] \cdot 3H_2O$ (see also Table 1). The reason for the small change is that the cyano ligand group only exhibits very weak bidentate character in PY.

Since PY and PB films only differ in the oxidation state of half the iron ions, the cyclic voltammetric response should be essentially identical. In Figure 3, the electrochemical response of a PY film between −200 and 1200 mV vs SCE is shown. The cyclic voltammogram shows two oxidation/reduction peaks with mid potentials of 250 and 770 mV comparable with PB. For the detailed position of the oxidation and reduction peaks, see Table 2. The origin of the additional reduction peak at 300 mV is not yet clear. It is possible that some material was leached out from the film during the voltammetric cycling so that the peak originates from the reduction of hydrated polyoxoiron(III) cations present in the aqueous solution at weakly acidic pH. The reversibility of the diagram is rather poor, possibly caused by the loss of some material during the first cycle.

3.3. Films of Nickel Hexacyanoferrate. Using the MSA technique, we also prepared films of nickel hexacyanoferrate in the reduced and oxidized form. They are denoted as $Ni^{II}HCF^{II}$ and $Ni^{II}HCF^{III}$ films, respectively. The $Ni^{II}HCF^{II}$ films were pale yellow with an absorption maximum at about 302 nm (Figure 2b), as typically found for the reduced form of nickel hexacyanoferrate.[6]

The $Ni^{II}HCF^{III}$ films were of a deeper yellow color, the UV/visible spectra showing a broad absorption band with maxima at 290 and 380 nm and a shoulder at 410 nm (Figure 2c), in agreement with spectra of the oxidized form of nickel hexacyanoferrate reported in the literature.[6] The lack of a charge-transfer band in the visible indicates that the Ni^{II}−NC−Fe^{III} sequence present in this complex salt only exhibits a weak mixed valence character. The insets in parts b and c of Figure 2 indicate that the absorbance increases nearly linearly with the number of dipping cycles—a clear indication that equal amounts of nickel hexacyanoferrate are deposited during each dipping cycle.

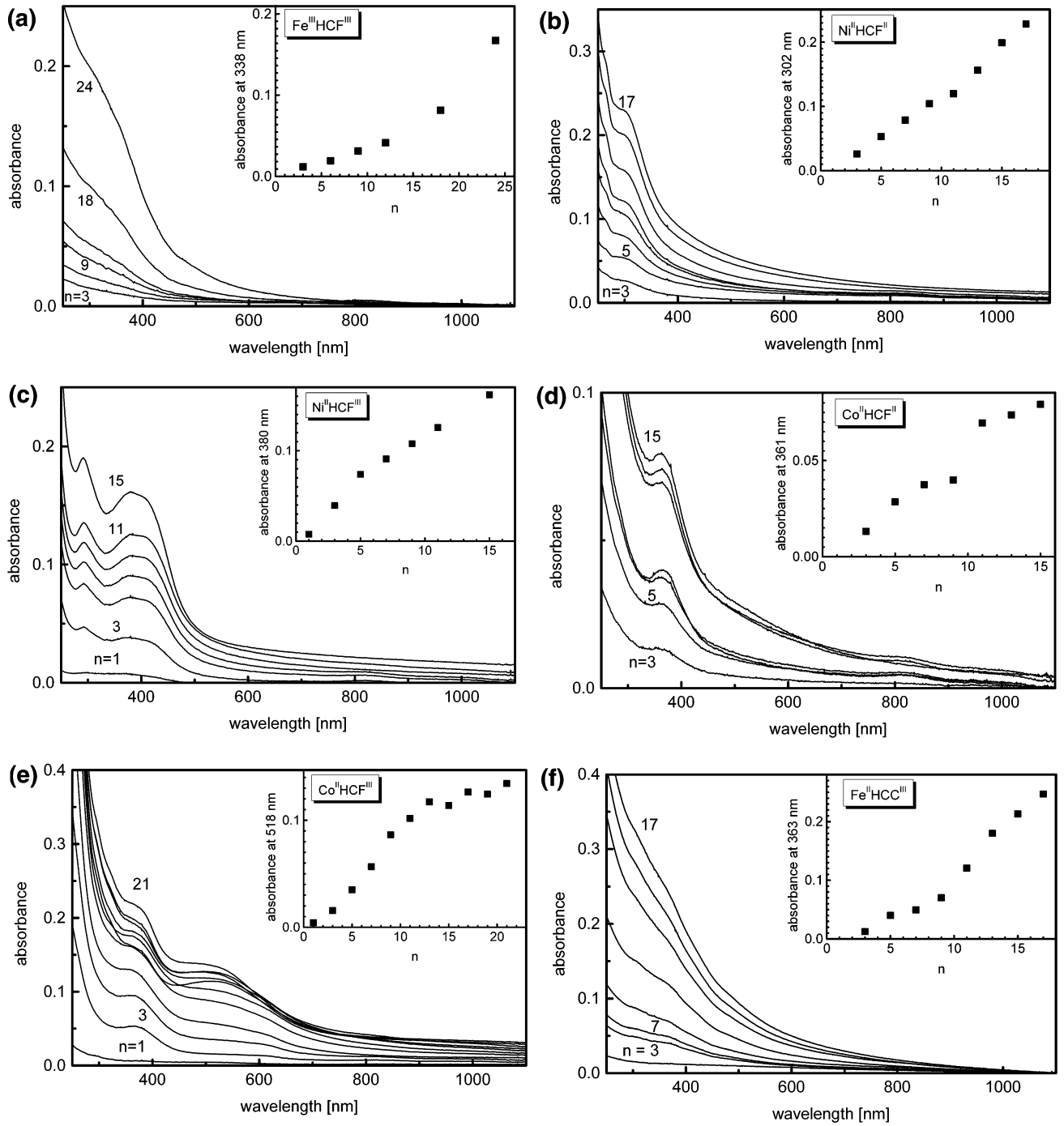

Figure 2. UV/visible absorption spectra of films of $Fe^{III}HCF^{III}$ (Prussian Yellow) (a), $Ni^{II}HCF^{II}$ (b), $Ni^{II}HCF^{III}$ (c), $Co^{II}HCF^{II}$ (d), $Co^{II}HCF^{III}$ (e), and $Fe^{II}HCC^{III}$ after various dipping cycles *n*. The insets show plots of the absorbance at selected wavelengths versus *n*. Substrates: Quartz plates coated with three layer pairs PSS/PAH.

The formation of the complex salt is also indicated in the infrared. FTIR spectra of $Ni^{II}HCF^{II}$ films exhibit a C−N stretching mode at 2086 cm^{-1}, whereas $Ni^{II}HCF^{III}$ films show two C−N stretching modes at 2094 and 2162 cm^{-1} (see also Table 1).

To study the electrochemical response, $Ni^{II}HCF^{II}$ films were deposited on ITO-coated glass substrates precoated with either a single layer of PDADMA or three layer pairs of PSS/PAH. Figure 4a shows typical voltammograms cycled between −200 and +1200 mV vs SCE. Two peaks occur which in their relative intensities are dependent on the kind of polyelectrolyte precoating. Let us first discuss the sample with PDADMA precoating. The reversible electrochemical behavior agrees well with electrochemically deposited nickel hexacyanoferrate films.[6,26,27] The strong peak with a mid-potential at 620 mV (vs SCE) is ascribed to the redox process of the iron center in the so-called soluble, potassium-rich modification of the complex salt according to eq 1,[6,26−28]

$$KNi''[Fe'''(CN_6)] + e^- + K^+ \rightleftharpoons K_2Ni''[Fe''(CN)_6] \quad (1)$$

whereas the shoulder with mid-peak potential at 470

(26) Vittal, R.; Gomathi, H. G.; Rao, P. *Electrochim. Acta* **2000**, *45*, 2083.
(27) Zeng, B.; Zhao, F.; Ding, X. *Anal. Sci.* **2001**, *17*, 259.
(28) Joseph, J.; Gomathi, H.; Rao, G. P. *Electrochim. Acta* **1991**, *36*, 1537.

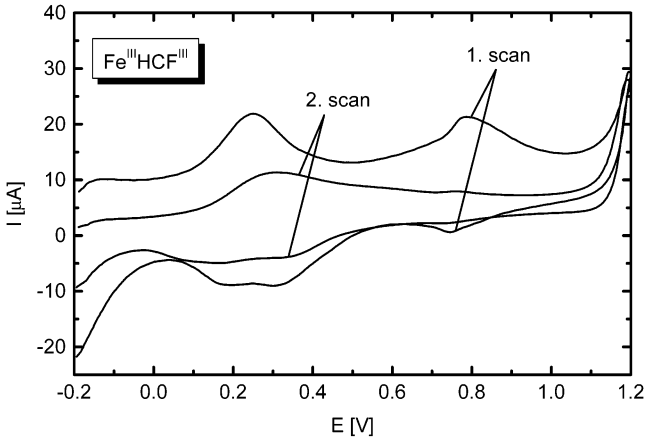

Figure 3. First and second voltammetric cycle of a freshly prepared $Fe^{III}HCF^{III}$ film using a potential range from −200 to 1200 mV vs SCE. Scan rate 2.3 mV s^{-1}, T = 20 °C. Substrate: ITO glass coated with a monolayer of PDADMA.

mV is related to the redox reaction of the iron centers in the potassium-free, so-called "insoluble" complex salt according to eq 2:[6,26−28]

$$Ni''_{1,5}[Fe'''(CN_6)] + e^- + K^+ \rightleftharpoons KNi''_{1,5}[Fe''(CN)_6] \quad (2)$$

The term "insoluble" only refers to the colloidal solubility of the complex salt. For the PSS/PAH precoated samples, two pronounced redox peaks with mid-potentials at 610 and 450 mV vs SCE are found (Figure 4a). For the detailed peak positions see Table 2. The peak positions are nearly identical with those of the sample precoated with PDADMA, but the relative height of the two peaks is very different. Therefore, it can be concluded that the substrate precoating plays an important role in the nucleation of the two modifications of $Ni^{II}HCF^{II}$. PDADMA with lower charge density than PAH favors the formation of the potassium-rich phase, possibly because electrostatic rejection of the potassium ions from the surface is less pronounced so that the concentration of K^+ ions near the film surface is higher.

The cyclic voltammogram of the $Ni^{II}HCF^{III}$ film on an ITO substrate precoated with three layer pairs PSS/PAH significantly differs from the diagram of the Ni^{II}-HCF^{II} film by showing a very broad oxidation peak ranging from 300 to 900 mV, and a reduction peak from 600 to almost 0 mV, respectively. The peak potential for oxidation is at 670 mV, and for the reduction at 270 mV (Table 2), the mid-potential being 470 mV vs SCE (Figure 4b). The high current during oxidation and reduction is striking. It is an order of magnitude higher than that for the $Ni^{II}HCF^{II}$ films and indicates a higher conductivity of the $Ni^{II}HCF^{III}$ films. The presence of additional, weakly pronounced shoulders of the oxida-

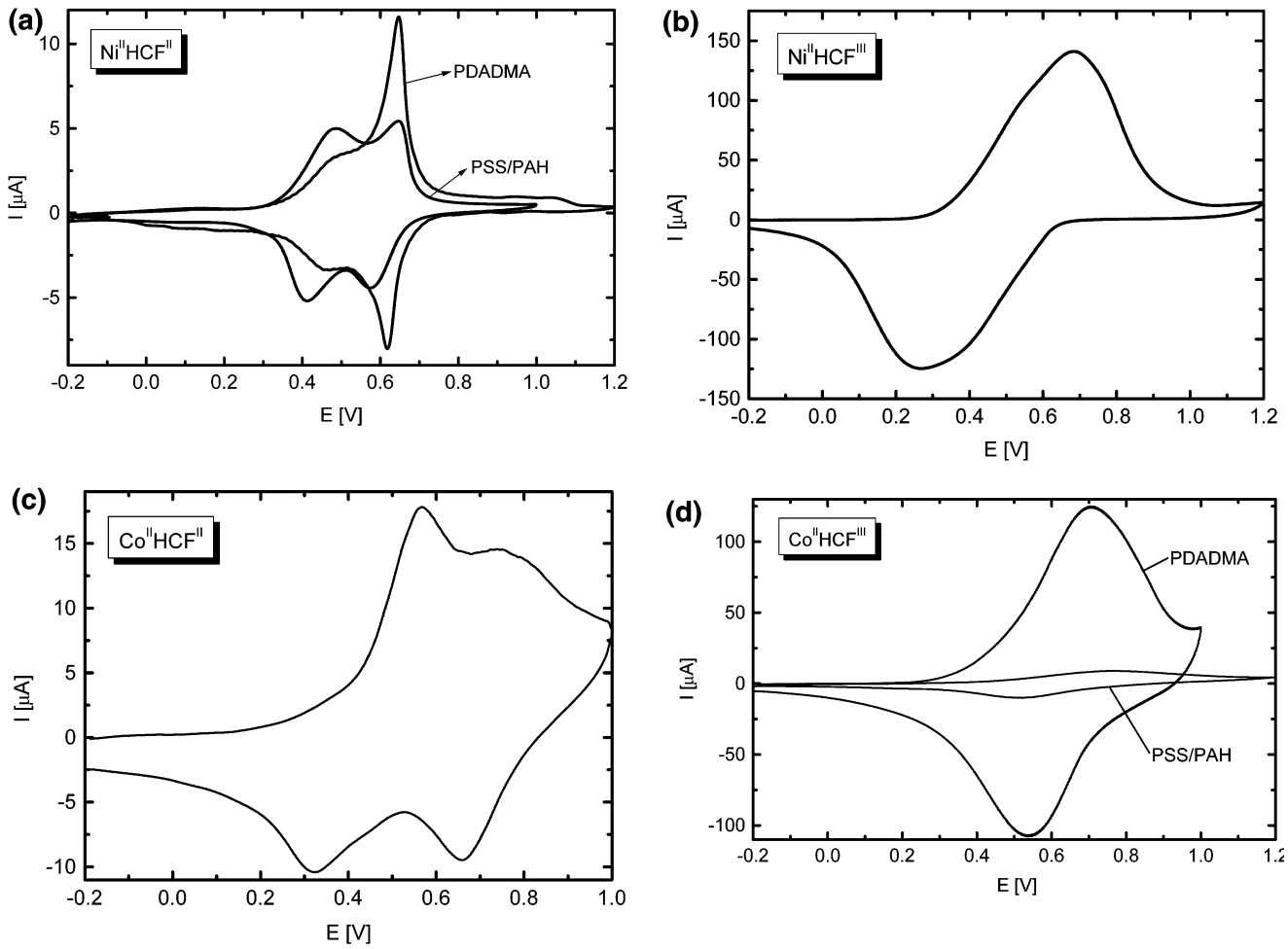

Figure 4. Cyclic voltammograms of films of $Ni^{II}HCF^{II}$ (a), $Ni^{II}HCF^{III}$ (b), $Co^{II}HCF^{II}$ (c), and $Co^{II}HCF^{III}$ (d) using a potential range from −200 to 1200 mV vs SCE. Substrates: ITO glass coated with a monolayer of PDADMA (a,c,d) or three layer pairs PSS/PAH (a,b,d). Scan rate 2.3 mV s^{-1}, T = 20 °C.

tion and reduction peaks can be ascribed to a heterogeneous structure of the film, very likely due to simultaneous presence of the potassium-containing and potassium-free modification. From the large width of the peaks it can be concluded that the phase separation is less complete so that oxidation/reduction and concomitant egress/ingress of potassium ions take place over a broad potential range.

3.4. Films of Cobalt Hexacyanoferrate. The MSA technique was also used to prepare films of cobalt hexacyanoferrate in the reduced and oxidized form. These films are denoted as $Co^{II}HCF^{II}$ and $Co^{II}HCF^{III}$ films, respectively. The $Co^{II}HCF^{II}$ film was of light brown color with an absorption maximum at about 361 nm (Figure 2d). UV/visible spectra are in agreement with spectra of the reduced form of cobalt hexacyanoferrate in the bulk phase.[29] Since cobalt and iron are present in the divalent state, any mixed valence charge-transfer band in the visible is missing. As shown by the plot in the inset of Figure 2d, the absorption at 361 nm increases rather irregularly with the number of dipping cycles. This indicates a rather heterogeneous film growth.

$Co^{II}HCF^{III}$ films were of purple-brown color, exhibiting a shoulder at 364 nm and an absorption maximum at 518 nm. The UV/visible spectrum in Figure 2e is in agreement with the visible spectrum of bulk cobalt hexacyanoferrate in the oxidized state.[29] The 518-nm absorption can be ascribed to the charge-transfer transition of the mixed valence Fe−CN−Co sequence. The inset of Figure 2e shows a plot of the absorbance at 518 nm against the number of dipping cycles. There is an almost linear increase in the absorbance up to about the 14th cycle, until the increase decelerates, indicating that now less material is adsorbed per dipping cycle.

The formation of the cobalt hexacyanoferrate complex salt is also indicated from the FTIR spectra of the self-assembled films. While $Co^{II}HCF^{II}$ films show a C−N stretching mode at 2080 cm^{-1}, the $Co^{II}HCF^{II}$ films exhibit a C−N stretching mode at 2109 cm^{-1}. This is somewhat in disagreement with electrochemically synthesized films, which show a C−N stretching frequency at 2088 cm^{-1} for the reduced state, and at 2142 cm^{-1} for the oxidized state.[23]

The electrochemical response of $Co^{II}HCF^{II}$ films was studied using cyclic voltammetry. Films adsorbed on ITO-coated glass pretreated with three PSS/PAH layer pairs were investigated. Figure 4c shows the reversible electrochemical behavior of the self-assembled $Co^{II}HCF^{II}$ film between −200 and +1000 mV vs SCE. The two peaks with mid-potentials at 450 and 720 mV can be ascribed to the oxidation/reduction of cobalt centers in the film.[23] For the detailed peak positions, see Table 2. The fact that two peaks occur may be related to the presence of the potassium-free and potassium-rich phase of the complex salt, as in the case of the $Ni^{II}HCF^{II}$ films discussed above.

The cyclic voltammogram of the $Co^{II}HCF^{III}$ film on an ITO-substrate precoated with a monolayer of PDADMA only shows a single, rather broad oxidation peak at 710 mV and a reduction peak at 540 mV (Figure 4d), the mid-potential of 630 mV being similar to those of films of the bulk material on graphite electrodes.[29] In the case of three layer pairs of PSS/PAH as precoating, the potentials are very similar (oxidation, 770 mV; reduction, 520 mV; mid-potential, 650 mV), but the peak currents are much lower, indicating an insulating effect of the polyelectrolyte precoating on the electroactive film. Any indication for a separation into the two modifications is missing. The diagrams are in agreement with those of electrochemically deposited films[23] or films of cobalt hexacyanoferrate particles precipitated from aqueous solution,[29] which also show a single signal for oxidation and reduction, respectively.

3.5. Films of Iron and Cobalt Hexacyanocobaltate. The MSA technique also allows unconventional combinations of ions so that films of little investigated hexacyanometalate complex salts such as $Fe^{II}HCC^{III}$ and $Co^{II}HCC^{III}$ can be easily prepared. $Fe^{II}HCC^{III}$ films are transparent and exhibit a brownish yellow color, whereas for the bulk material an ivory yellow color is reported.[30] In Figure 2f UV/visible spectra of the films are shown, indicating a strong absorption in the UV with a long-wavelength tail extended to the visible. A charge-transfer band in the visible is lacking. The weak shoulders at 363 and 500 nm may be ascribed to the presence of small amounts of $Co^{II}HCF^{III}$ (see also Figure 2e), which might have formed upon an exchange of some of the cobalt and iron sites in the film. As indicated in the inset of Figure 2f, the absorbance at 363 nm increases with the number of dipping cycles, but the increase is nonlinear, indicating a heterogeneous film growth. The formation of the complex salt is also evident from infrared spectra. While the C−N stretching mode of the cyano ligand in potassium hexacyanocobaltate-(III) appears at 2143 cm^{-1},[31] it is shifted to 2161 cm^{-1} in the $Fe^{II}HCC^{III}$ films assembled on a glass substrate (Table 1), similar to the value of 2168 cm^{-1} reported for the bulk material.[31] Cyclic voltammetric studies of an $Fe^{II}HCC^{III}$ film on a PDADMA-coated ITO substrate do not indicate reversible oxidation/reduction peaks in the potential range between −200 and 1200 mV vs SCE.

We also tried to prepare transparent films of cobalt-(II) hexacyanocobaltate(III). However, the alternate dipping of substrates into 0.1 M aqueous solutions of Co(II) and HCC(III) ions only led to pinkish, microcrystalline deposits on the substrate and the use of less concentrated, 10^{-2} M solutions was quite unsuccessful for film deposition. FTIR spectra of the $Co^{II}HCC^{III}$ films indicate a C−N stretching mode at 2172 cm^{-1}.

3.6. Ion Separation of Membranes. To study the ion transport across PB-type films, we prepared Fe^{III}-HCF^{II} membranes on porous polymeric supports using the MSA technique. Details of the membrane preparation are given in the experimental part. Since the ion separation originates from the size-selective ion flow through the zeolitic channels of the PB-type lattice, it is very important to prepare a dense, defect-free separating membrane not showing nonselective transport

(29) Kulesza, P.; Malik, M. A.; Berrettoni, M.; Giorgetti, M.; Zamponi, S.; Schmidt, R.; Marassi, R. *J. Phys. Chem. B* **1998**, *102*, 1870.

(30) de Robertis, A.; Bellomo, A.; de Marco, D. *Talanta* **1976**, *23*, 732.

(31) Inoue, H.; Fluck, E.; Yanagisawa, S. *Z. Naturforsch.* **1976**, *31b*, 167.

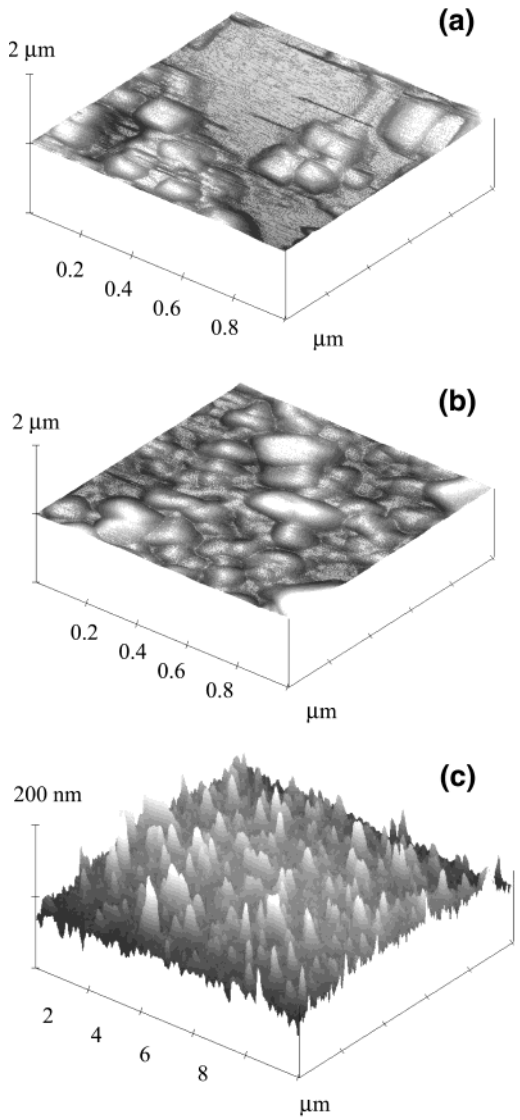

Figure 5. SFM perspective images of $Fe^{III}HCF^{II}$ on quartz substrates precoated with three layer pairs PSS/PAH after 10 (a) and 20 (b) dipping cycles and of a $Co^{II}HCF^{III}$ separating membrane on a porous support after 60 dipping cycles (c).

through defects and voids. Preliminary SFM studies of $Fe^{III}HCF^{II}$ films on precoated quartz supports indicated that they consist of a multitude of small crystallites of about 50−150 μm in diameter. While after 10 dipping cycles the substrate surface was not yet continuously covered with crystallites, the use of 20 dipping cycles was sufficient to achieve a complete coating (Figure 5a,b). From the SFM study it was clear that a dense, defect-free separating membrane could only be obtained if at least 20, perhaps even more, dipping cycles were applied. We therefore prepared three membranes with 20, 60, and 100 dipping cycles and studied the transport of various aqueous electrolyte salts across these films. The ion transport was investigated using conductivity measurements as described in the experimental part. In Figure 6, the flux of various electrolyte salts across the three $Fe^{III}HCF^{II}$ membranes is plotted versus the Stokes radii r_h[32] of the corresponding hydrated cations. If the dominating transport mechanism is ion sieving

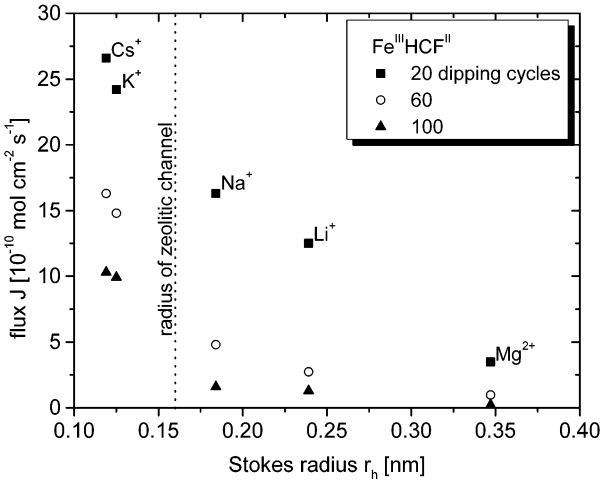

Figure 6. Plot of flux J of various electrolyte salts across Fe^{III}-HCF^{II} membranes as a function of the Stokes radius r_h of the metal cations and the number of dipping cycles.

by the zeolitic structure of PB, one has to expect much lower flux values for cations with r_h values being larger than 0.16 nm, the channel radius of the PB lattice. However, for the sample with 20 dipping cycles, relatively high flux values of the electrolyte salts were found, which only gradually decreased with increasing cation radius r_h. Selectivities α(CsCl/NaCl) and α(KCl/NaCl) were only 1.6 and 1.5, respectively. Thus, a clear indication for ion sieving was lacking, probably because the separation layer was too thin and not free of defects. However, for the sample with 60 dipping cycles the expected sudden drop of the ion flux at an r_h value of 0.16 nm occurred: While Cs^+ and K^+ ions with r_h values of 0.119 and 0.125 nm[32] easily passed the membrane showing high flux values, Na^+, Li^+, and Mg^{2+} ions were hindered and only showed low J values. Their r_h values of 0.184, 0.239, and 0.347 nm,[32] respectively, are larger than the zeolitic channels so that they can penetrate the PB lattice only after they become partially dehydrated. Consequently, the selectivities were improved; the α(CsCl/NaCl) and α(KCl/NaCl) values were 3.4 and 3.1, respectively. The effect of ion sieving was most pronounced for the thickest membrane subjected to 100 dipping cycles. For this membrane, high α(CsCl/NaCl) and α(KCl/NaCl) values of 6.5 and 6.2 were observed. The results indicate that with an increasing number of dipping cycles the concentration of defects and voids spanning the whole membrane decreases so that the ion transport is more and more dominated by selective permeation through the channels of the PB lattice, and nonselective transport across the defect sites is progressively prevented. It should be pointed out that the α values clearly exceed the selectivities determined for self-assembled polyelectrolyte multilayer membranes (α(KCl/NaCl) = 1.5 for 60 layer pairs of PVA/PVS[33−35]) and for ionophore-containing polymer membranes especially designed for alkali-metal separation, the ionophores being matrix-fixed crown ethers (α(KCl/NaCl) ≤

(32) Pau, P. C. F.; Berg, J. O.; McMillan, W. G. *J. Phys. Chem.* **1990**, *94*, 2671.

(33) Krasemann, L.; Tieke, B. *Langmuir* **2000**, *16*, 287.

(34) Harris, J. J.; Stair, J. L.; Bruening, M. L. *Chem. Mater.* **2000**, *12*, 1941.

(35) Toutianoush, A.; Tieke, B. In *Novel methods to study interfacial layers*; Möbius, D., Miller, R., Eds.; Elsevier: New York, 2001; p 415.

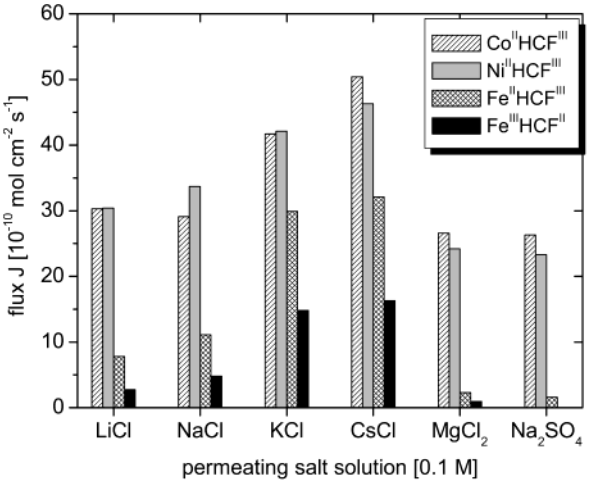

Figure 7. Flux *J* of various alkali-metal chlorides, magnesium chloride, and sodium sulfate across self-assembled membranes of $Fe^{III}HCF^{II}$, $Fe^{II}HCF^{III}$, $Ni^{II}HCF^{III}$, and $Co^{II}HCF^{III}$. Membranes were prepared upon 60-fold alternate dipping of the porous PAN/PET support into the corresponding solutions.

2.1[36,37]). For PB-type membranes under electroless conditions, comparable data have not been published yet.

In addition to the $Fe^{III}HCF^{II}$ membranes we also studied the ion transport behavior of the analogous $Co^{II}HCF^{III}$, $Ni^{II}HCF^{III}$, and $Fe^{II}HCF^{III}$ membranes. A surface view of a $Co^{II}HCF^{III}$ membrane is shown in the SFM image of Figure 5c. It indicates that after 60 dipping cycles a complete coverage of the supporting membrane with a multitude of crystallites is obtained and a continuous separating membrane is formed. The flux values of various alkali-metal chlorides, magnesium chloride, and sodium sulfate across the membranes are compiled in Figure 7. It is striking that the membranes showed higher flux values for all electrolyte salts than the $Fe^{III}HCF^{II}$ membranes. First of all, this can be ascribed to a lower thickness of these membranes: The lower charge number of the adsorbed ions causes less material to be adsorbed per dipping cycle than in the $Fe^{III}HCF^{II}$ membranes and thus the membranes are more defective. From the optical spectra in Figure 1 it can be derived that after an equal number of dipping cycles, the $Fe^{II}HCF^{III}$ films contain 25% less material than $Fe^{III}HCF^{II}$ films. Consequently, after 60 dipping cycles the selectivity α(KCl/NaCl) of an $Fe^{II}HCF^{III}$ membrane was only 2.7.

In the case of the cobalt- and nickel-based membranes, the simultaneous presence of a potassium-rich and a potassium-free phase may additionally account for the transport behavior. The presence of two phases implies additional phase boundaries favoring additional defects in the membrane. To date, the simultaneous presence of two modifications of cobalt and nickel hexacyanoferrate is only apparent from spectroscopic and cyclic voltammetric studies,[23,29,38] whereas morphological investigations on their local distribution and on the presence of relevant defects are still lacking. Despite these problems the cobalt- and nickel-containing membranes still exhibit an enhanced flux for cations with small Stokes radii such as Cs^+ and K^+. The selectivities α(CsCl/NaCl) and α(KCl/NaCl) of the $Co^{II}HCF^{III}$ membrane subjected to 60 dipping cycles are 1.7 and 1.4, for example. For the $Ni^{II}HCF^{III}$ sample the same α values were found. The lower flux of sodium sulfate compared with sodium chloride can be ascribed to anion sieving because the sulfate ion is much larger than the chloride ion and thus is excluded from the zeolitic channels.

4. Conclusions

Our study shows that the method of multiple sequential adsorption of metal cations and hexacyanometalate anions provides an easy access to films of polynuclear transition metal cyanides with monolayer precision. It is demonstrated that films of metal hexacyanoferrates can be directly prepared in different oxidation states of the metal cation and the hexacyanometalate anion. For example, films of PB, Prussian White (Everitt's salt), and PY could be directly prepared. It is also demonstrated that the film formation is affected by the charge number of the ions. In the case of PB the use of trivalent metal cations and tetravalent hexacyanoferrate anions leads to higher surface coverage than the use of divalent metal cations and trivalent anions. Moreover, the nature of the substrate precoating has a strong effect on morphology and electrochemical response of the films of the complex salts. This originates from different charge densities as well as conductivities of the substrates. In the case of nickel hexacyanoferrate, the charge density of the substrate influences the ratio, to which the potassium-free and potassium-containing modifications are formed. In the case of cobalt hexacyanoferrate, the peak current during cyclovoltammetric cycling was strongly influenced. The method of multiple sequential adsorption even allows preparation of films of unusual complex salts such as iron and cobalt hexacyanocobaltate.

In general, the self-assembled films are colored and electroactive and can be switched between different oxidation states of the metal ions and might be useful as electrochromic displays or catalytic surfaces. Because of the choice of different combinations of ions, the electrochemical and electrochromic behavior of the films can be widely tailored.

Especially the alternating adsorption of ferric cations and tetravalent hexacyanoferrate anions leads to densely packed and defect-free films, which can be used as ion-sieving membranes utilizing the zeolitic structure of the PB crystal lattice. Our preliminary studies of permeation of alkali-metal chlorides across the films indicate high separation factors α for cesium chloride and sodium chloride, or potassium chloride and sodium chloride. The α-values of 6.5 and 6.2, respectively, exceed those of self-assembled polyelectrolyte multilayer membranes,[34−36] in which the ion separation is based on different charge densities of the permeating ions and those of ionophore-containing polymer membranes, the ionophores being matrix-fixed crown ether-type compounds.[37,38] However, membranes prepared from PB analogues such as cobalt and nickel hexacyanoferrate were found to be less suited for ion separation. This is first due to the lower charge numbers of the adsorbed ions ($z^+ = 2$, $z^- = 3$), which

(36) Thunhorst, K.; Noble, R. D.; Bowman, C. N. *J. Membr. Sci.* **1999**, *156*, 293.
(37) Beginn, U.; Zipp, G.; Möller, M. *Adv. Mater.* **2000**, *12*, 510.
(38) Jeerage, K. M.; Steen, W. A.; Schwartz, D. T. *Chem. Mater.* **2002**, *14*, 530.

cause less material to be adsorbed per cycle so that the membranes are thinner and more defective. In addition, the heterogeneous structure of these films consisting of a potassium-containing and potassium-free modification may also play a role. Additional phase boundaries are present in these films, which likely cause a higher defect concentration. Presently, a more detailed study on the growth and the morphology of the PB-type films and its relevance to the ion transport behavior is carried out, which will be published elsewhere.[39]

(39) Pyrasch, M.; Schnepf, J.; Jin, W.; Toutianoush, A.; Tieke, B., in preparation.

Acknowledgment. Dr. A. Hübner, Sulzer Chemtech, Neunkirchen, is gratefully acknowledged for supplying plasma-treated PAN/PET supporting membranes. Prof. W. Rammensee and Dr. B. Simons (Universität zu Köln, Institut für Mineralogie und Geochemie) are thanked for kindly allowing us to use their scanning force microscope and for helpful discussions. One of us (W. Jin) thanks the Alexander von Humboldt foundation for a scholarship. The Deutsche Forschungsgemeinschaft is thanked for financial support (Project Ti 219/6-2 and 7-1).

CM021230A